

EVALUATING THE USE OF REMOTE SENSING FOR LAND COVER  
CLASSIFICATION AND MONITORING OF A SHIFTING ECOSYSTEM

A Thesis

Presented to

The Faculty of the Environmental Program

The Colorado College

In Partial Fulfillment of the Requirements for the Degree

Bachelor of Arts in Environmental Science

By

Frannie Nelson

May 2021



---

Dr. Charlotte G. Gabrielsen

Assistant Professor of Environmental Science, Colorado College



---

Dr. Miroslav Kummel

Associate Professor of Environmental Science, Colorado College

# TABLE OF CONTENTS

ABSTRACT .....	2
ACKNOWLEDGEMENTS.....	3
INTRODUCTION .....	4
ECOSYSTEM SHIFTS UNDER CLIMATE CHANGE .....	4
ALASKA AS A MODEL STUDY SYSTEM.....	5
REMOTE SENSING AS A TOOL TO MONITOR ECOSYSTEMS .....	9
OBJECTIVES .....	10
METHODS .....	11
STUDY AREA .....	11
IMAGE COLLECTION AND PROCESSING .....	12
AERIAL ORTHOIMAGERY CLASSIFICATION .....	14
GROUND-TRUTH DATA COLLECTION .....	15
CLASSIFICATION ACCURACY ASSESSMENTS .....	16
RESULTS .....	18
LAND COVER CLASSIFICATION ACCURACY .....	18
ACCURACY ASSESSMENT OF AGGREGATED VS. NON-AGGREGATED CLASSIFICATIONS .....	19
COVERAGE OF CLASSIFIED LAND COVER CLASSES .....	20
DISCUSSION.....	21
ACCURACY OF LAND COVER CLASSIFICATIONS .....	21
EFFECT OF SPATIAL AGGREGATION ON CLASSIFICATION ACCURACY .....	22
GROUND-TRUTHED VS. IMAGE-BASED VALIDATION APPROACHES.....	23
IMPLICATIONS OF LAND COVER CLASS COMPOSITION .....	26
RECOMMENDATIONS FOR AERIAL IMAGERY CLASSIFICATION EFFORTS .....	30
FUTURE DIRECTIONS .....	32
CONCLUSION.....	33
REFERENCES .....	35
TABLES AND FIGURES .....	44

## ABSTRACT

Contemporary climate change in Alaska has caused amplification and unpredictability in disturbance regimes that drive ecosystem function. As a result, many ecosystems across the Boreal and Arctic regions are undergoing abrupt transitions that are recharacterizing landscape patterns, ecological processes, species composition, structure, and trophic biophysical interactions. In this study, I used remote sensing and spatial analyses to classify a dynamic ecosystem in the Caribou Hills Grassland region of Alaska's Kenai Peninsula, USA. This region is currently undergoing a shift from a historical boreal spruce forest to a savannah-like system as a result of an extensive spruce bark beetle outbreak in the 1990s through the early 2000s that killed thousands of acres of trees, followed by a rapid and intense human-caused fire that burned about 56,000 acres in 2007. To characterize the landcover of the Caribou Hills and develop a protocol for monitoring future landcover transitions, I collected two sets of aerial imagery in 2019 and 2021, each collected at a separate spatial resolution and time of year, and used a maximum likelihood classification approach to classify the dominant land cover types (grass, shrub, and spruce). Overall, classification accuracies across both images were above 78%, and I found that the Caribou Hills landscape is currently comprised, on average, of 67% grass, 27% shrub, and 3% spruce. Assessing post-disturbance succession and ecosystem transitions requires long-term monitoring. Because the Caribou Hills Grassland region is large and remote, frequent monitoring through aerial imagery will be valuable for assessing land cover change over time. As the management of shifting ecosystems is relatively new to land managers, approaches such as the one developed in this study can be used as guidance towards innovative monitoring efforts and land stewardship.

## ACKNOWLEDGEMENTS

Throughout the process of research design, collection, processing, analyzing, and writing this thesis, I have received valuable help from my mentors and peers.

First, I would like to thank my thesis advisor and mentor, Dr. Charlotte Gabrielsen, for advising me through all of these steps; for being supportive and encouraging; and for challenging me and teaching me so much about this process. She helped me troubleshoot, critically think, and navigate the obstacles that this study brought about. She has also been incredibly patient and consistent with me since I first came to her about my thesis two years ago.

I would also like to thank the Kenai National Wildlife Refuge, especially Mark Laker, Dawn Magness, Kris Inman, and my fellow biological technicians for collaborating and providing insight into research design and for making data collection possible both in the air and on the ground. I am incredibly thankful to Mark Laker for teaching and training me in remote sensing, processing, and for playing a key role in acquiring both sets of imagery used in this thesis. I would also like to acknowledge the GIS Lab and the Environmental Program at Colorado College, particularly Matt Cooney and Dr. Miro Kummel, for their guidance, input, and assistance. Finally, I could not have gotten through this thesis without the enthusiasm and optimism from my roommates and thesis student cohort.

## INTRODUCTION

### *Ecosystem shifts under climate change*

Climate change has the potential to alter ecosystem structure and function through largescale changes to disturbance regimes (Buma, 2015; Malhi et al., 2020). As disturbance regimes of ecosystems are altered, they are more likely to transition into new ecosystems characterized by different landscape patterns, ecological processes, and species (Gonzalez et al., 2010). These ecosystem shifts involve complex interactions, causing diverse effects to ecosystem dynamics, structure, function, species composition, and biophysical interactions across entire biomes. Changes in climate can impact vegetation mortality and recruitment (Gonzalez et al., 2010). For example, if vegetation in a given ecosystem is not acclimated to drought, warmer temperatures, or increased fire or other disturbance, increased rates of mortality and decreased recruitment may cause shifts in the dominant vegetation towards species that can thrive under these new climate conditions (Gonzalez et al., 2010).

Under current climate change, biomes and the species that comprise them are, as a general trend, moving latitudinally and in increasing elevation to stay within their climate envelopes (Gonzalez et al., 2010). While many species are capable of adapting to new environmental conditions, feedback loops between natural processes and human-induced warming may amplify climatic impacts that exceed species' physiological thresholds (Mann et al., 2012). For example, carbon cycling and albedo are strongly controlled by warming temperatures and vegetation cover, which in turn dictate energy absorption at the surface (Gonzalez et al., 2010). With increases in atmospheric carbon and decreased albedo, atmospheric temperature and landcover may experience significant alterations (Gonzalez et al., 2010). As

ecological tipping points are being reached and climate change is further intensified, some ecosystems may be permanently altered, while others may prove to be more resistant to change (Gonzalez et al., 2010).

An ecosystem shift – the transition of an ecosystem from one type to another – is considered to represent an “abrupt change in an ecological system” (ACES). Disturbances interacting with each other or with climate can also generate ACES (Turner et al., 2020). It is important to consider the variables, processes, and events that may be important in driving ecosystem shifts (Chapin & Starfield, n.d.). To determine the relevant drivers of ecosystem shifts, there is a critical need for place-based studies in order to identify the mechanisms and factors impacting particular regions, which in turn can be more easily incorporated into potential ACES monitoring or modeling efforts. Furthermore, accurately modeling and predicting environmental trajectories is challenging, particularly for ecosystems that are experiencing rapid ecological change. For these ecosystems, precedent conditions and regimes are often unknown. Accordingly, there is a need to invest more energy into developing innovative approaches for capturing long-term data and sustaining process-focused data collection.

#### *Alaska as a model study system*

Alaska represents an ideal location to explore the effects of climate change on ecosystem shifts, as the region is experiencing warming faster than any other part of the globe (Mann et al., 2012). Interior Alaska has experienced an increase of 1.4°C in the last century compared to 0.8°C worldwide (Wendler et al., 2009). Precipitation has decreased by 11%, and since the 1970’s, the growing season has increased by 3 days per decade, resulting in earlier spring onset and frost occurring later in the fall. Permafrost temperatures have increased by 2-4°C in the past 50-100 years (Hinzman et al., 2005) and American Arctic glaciers have experienced among the greatest

mass loss, many displaying 30% reductions in just 40 years (Hinzman et al., 2005). In combination, these climatic alterations are causing cascading effects to ecosystem structure and function (Box et al., 2019). Warmer temperatures and drought are causing not only longer growing seasons and land and sea ice melt, but increased disturbances such as wildfire, abrupt permafrost thaw, and more frequent and intense insect outbreaks (Box et al., 2019; Grimm et al., 2013). These physical disturbances may alter tree density, expansion of shrub biomass trees into tundra, or shifts in vegetation. Changes in tree density in combination with permafrost thaw play a key role in carbon uptake, cycling, local hydrology, in turn leading to changes in species distributions across both aquatic and terrestrial ecosystems (Box et al., 2019; Grimm et al., 2013).

Alaska is comprised largely by boreal forests which collectively store more than one third of terrestrial stored carbon stocks, making them key contributors to carbon cycling (Bradshaw & Warkentin, 2015). Boreal forests have historically served as important carbon sinks, being responsible for significant carbon uptake during the Last Glacial Maximum (19-26.5 kyr ago; Bradshaw & Warkentin, 2015). However, as a result of deforestation and rapid temperature increases in the Arctic, it appears that these sinks may be weakening (Stephens et al., 2007; Bonan, n.d.; Hayes et al., 2011). Furthermore, boreal forests contain more freshwater than any other biome and contribute to climate regulation through water and energy cycling (Baughman et al., 2020). Increased climate stress and disturbance from deforestation may further promote ecosystem shifts (Baughman et al., 2020; Peng et al., 2011; Soja et al., 2007). In addition to impacts to ecosystem services, increased disturbance is predicted to cause extensive habitat loss (Hess et al., 2019).

Ecosystem shifts have the potential to impact Alaska's economy and global carbon sinks. Alaska's economy is primarily based on natural resource extraction; federal, civilian, and military spending; and tourism (BEA 2018; Goldsmith 2010; McDowell 2016). Oil production, commercial fishing, and nature-based tourism make up a large portion of Alaska's economy and may all be affected by ecosystem shifts (Berman et al., n.d.). Furthermore, subsistence is a prominent practice in both tribal and non-tribal communities in the Arctic, emphasizing the need to maintain valuable subsistence species. Emblematic species will be forced to migrate to new ecosystems that meet their habitat needs. Exploring the best ways to monitor and manage these anticipated changes is important to consider in an effort to increase understanding of ecosystem shifts in the Arctic (Melvin, 2019).

Alaska has a large percentage of protected areas, including a diverse network of lands managed by the Federal Refuge system. As a result of numerous abrupt system-wide shifts, conservation of these unique ecosystems has proven challenging. As climate envelopes and ecosystems move, collaborating with land managers and other agencies to bolster connectivity and linkages between protected lands could help species to migrate or maintain diversity in species and habitat (Bernhardt & Leslie, 2013). Additionally, targeting species or areas of particular known resilience for reserves or refuges may also help to maintain greater function and diversity (Bernhardt & Leslie, 2013).

The Kenai Peninsula of Alaska is particularly well-suited for addressing questions related to ecosystem shifts. The Kenai Peninsula was settled by the Dena'ina and Alutiiq people around 1000 A.D. who practiced subsistence (Baughman et al., 2020). The region was then colonized by Russia and the United States in the late 17th and 18th centuries, where fisheries, fur trade and fox farming took off (Baughman et al., 2020). Homesteading increased after gold, oil and gas were later discovered in the late 1800s. In response to the discovery of these resources, increased



human development, road construction, agriculture or city infrastructure has greatly altered land cover and risk of human-caused wildfire (Baughman et al., 2020). The Kenai Peninsula is also one of Alaska's largest sectors for nature-based tourism, contributing approximately 175 million USD as found in 2016 (Baughman, 2020).

With increased warming, drought, and human population, fire and spruce bark beetle (SBB) outbreak intensity is projected to increase and shorten intervals, in turn causing major landscape shifts in this region. In the 1990s through the early 2000s, an extensive SBB outbreak across the Caribou Hills on the Kenai Peninsula killed thousands of acres of trees, causing up to 87% mortality in some areas (Hess et al., 2019). In 2007, a rapid and intense human-caused fire burned about 56,000 acres (Kenai Peninsula Borough, 2007). Typically, SBB outbreaks would occur every couple of decades on the Kenai Peninsula when colder temperatures could regulate SBB populations. However, warming has been found to influence SBB population size through increased overwinter survival, larval maturation, and increased drought-induced stress on mature host trees which weakens their natural defense tactics against SBB (Berg et al., 2006; Hess et al., 2019). Endemic levels of SBB populations will be high enough to perennially thin forests. While SBB outbreak, independently, has not been shown to significantly increase wildfire susceptibility, its increasing presence on the Kenai Peninsula, in correlation with shifts towards a grassland-like system, may create conditions similar to the surface fuel ignition typical of boreal forests (Hess et al., 2019). Full boreal systems typically have fire intervals of 79 years which is much shorter than the Kenai Peninsula's historical 400-600 year interval (Berg & Anderson, 2006). It is speculated that shorter fire intervals, in addition to increased SBB disturbance, will only further promote this ecosystem shift. While preliminary observations show the beginning of a major ecosystem shift, the Caribou Hills are very familiar with disturbance and may show substantial resilience and plasticity despite intensification and changes in climate.

### *Remote sensing as a tool to monitor ecosystems*

The ability to monitor and describe the dynamics of shifting ecosystems has become increasingly possible with advances in remote sensing and Geographic Information Systems (GIS) technology. Detection and investigation of change in ecosystems using aerial imagery allows managers to monitor landscape dynamics over large areas, including those that are hazardous or difficult to access. Furthermore, it facilitates the extrapolation of costly ground measurements (Kennedy et al., 2009; Li et al., 2003; Petersen et al., 2005; Schuck et al., 2003). As climate change acts not only on specific species, habitats or ecosystem characteristics, it also acts across landscapes of much greater spatial extents; in turn, larger-scale studies are often required (Kerr & Ostrovsky, 2003). Traditional ecological field studies do not translate readily to regional or global extents as they are often time consuming, expensive, and restricted by access (Kerr & Ostrovsky, 2003). Remote sensing technology, in the form of aerial imagery or satellite imagery, can capture consistent measurements of landscape condition, allowing detection of both abrupt changes or slow trends over time (Kennedy et al., 2009). Furthermore, remotely based measurements can be used in conjunction with field work to gather large scale data and develop a valuable understanding of changing ecosystems. Remote sensing allows for the collection of a large range of ecological and biological metrics and observations, including details of habitat type (*e.g.*, land cover classification) and their biophysical properties (*e.g.*, integrated ecosystem measurements), as well as the ability to detect natural and human-induced changes across landscapes (change detection; Kerr & Ostrovsky, 2003).

Multispectral imagery (Red, Green, Blue, LWIR, NIR) of varying resolutions can be leveraged to differentiate land cover and produce land cover classifications, providing the basis to address numerous important ecological questions. Classifications may be spectral-based

supervised and unsupervised, or object-based, which uses both spatial and spectral data to determine land cover composition. Peterson et al (2005), for example, used spectral aerial imagery to classify willow species in southeastern Oregon. Furthermore, Iverson (1989) showed that the long (30-year) temporal archive of imagery offered by satellites such as Landsat could be used to delineate land-use changes, including conversion of forests for urban or agricultural development (Cohen et al., 2007; Hansen et al., 2013; Iverson et al., 1989). Landsat imagery over the state of Alaska has been used to make observations of shrub expansion; coastal erosion and alterations in wetting/drying trends; increased thermokarst from warm and wet summers; glacial retreat from rising temperatures, declining snowfall, and mechanical processes; as well as fire/SBB regimes and post-fire/SBB productivity with feedback implications (Pastick et al., 2019). Classifications of remotely sensed imagery can provide researchers and land managers with a strong sense of ecosystem dynamics, enabling timely management of biodiversity. Additionally, spatial analysis of trees can offer important insights into recruitment dynamics, which are of increasing interest to ecologists studying rapid changes in climates.

### *Objectives*

In this study, I sought to develop an approach to classify land cover from aerial imagery collected in the Caribou Hills grassland region on the Kenai Peninsula, Alaska, United States. The main objectives of this research were to: (1) create an efficient workflow to collect, process, and analyze aerial imagery to generate accurate land cover classifications; (2) assess the effect of image acquisition variables, including time of year, weather, spatial resolution and extent, on classification accuracy; and (3) evaluate the utility of remote sensing technologies for monitoring ecosystem transitions and informing adaptive management strategies.

To date, few studies exploring landscape delineation and recruitment have been conducted in

ecosystems that have experienced disturbance intensity and rates of change as high as in the Caribou Hills. This research will be valuable in not only developing an approach to identify patterns of spruce recruitment in the grassland, but to provide information relevant to the conservation and management of landscapes susceptible to ecosystem shifts under projected climate change, which in turn will promote biodiversity and resilience (Melvin, 2019).

## METHODS

### *Study area*

This study was conducted in the Caribou Hills region, located on the Kenai Peninsula in south-central Alaska, United States (Fig. 1). The Kenai Peninsula lies between Cook Inlet and Prince William Sound and consists of the Gulf Coast, Kenai Mountains, and Kenai Lowlands ecoregions. This region represents a transitional maritime environment situated between coastal rainforests and boreal forests of the arid Interior of Alaska (Berg & Anderson, 2006). Its position between biomes results in many of the key landcover components of Arctic, sub-Arctic, Boreal, and coastal ecosystems being situated within close range of one another (Baughman et al., 2020). The Kenai Peninsula also has a relatively dense human population, relative to the rest of the state (Morton et al., 2006).

The Caribou Hills region comprises a roughly 40,000-acre grassland along the southern Kenai Lowlands between Homer and Ninilchik. The area consists of a broad plateau of hilly morainal belts, flat glacial lake beds, outwash plains, and multi-terraced river channels, with elevations generally ranging from 15 to 100 m (Berg & Anderson, 2006). Dominant vegetation includes black spruce (*Picea mariana*), paper birch (*Betula neoalaskana*), Kenai birch (*Betula kenaica*), white spruce (*Picea glauca*), quaking aspen (*Populus tremuloides*), and Lutz spruce

*Picea x lutzii*). The area historically had fire intervals of 400-600 years, with spruce bark beetle (SBB) outbreaks occurring up to 10 times in between (Berg & Anderson, 2006).

### *Image collection and processing*

Color-infrared aerial photographs of the Caribou Hills Grassland region were collected in two separate years: 2019 and 2021 (Fig. 1). Aerial imagery collected in 2019 encompassed a spatial extent of 251 km<sup>2</sup> with a spatial resolution of 0.1 m (10 cm; Fig. 2), whereas the 2021 imagery encompassed a smaller spatial extent of 38 km<sup>2</sup>, but a much finer spatial resolution of 0.05 m (5 cm; Fig. 3). The 2021 imagery was collected in a single day across a 3-hour period. However, because the spatial extent of the image collection was much larger in 2019, imagery was collected over the span of two days. To investigate if the timing of imagery acquisition would affect the ability to delineate between vegetation types, imagery from each year was collected at different times across the growing season. In 2019, imagery was collected in May when the grass was khaki-colored, shrubs were dark-brown, and spruce trees were green. In 2021, on the other hand, imagery was collected in August when vegetation classes appeared more similar in color.

The 2019 imagery was acquired using two Nikon D810 cameras mounted aboard a CubCrafters CC18 Top Cub aircraft. One camera was unmodified and collected red/green/blue (RGB). The other camera was modified by Maxmax.com to collect in the infrared spectrum (> 715) by removing the cameras infrared cut filter. In 2021, the LUCINT12 multispectral imaging system was mounted on a rack below the aircraft. The LUCINT12 had an array of cameras that simultaneously captured RGB, IR, Red Edge (RE), and long-wave infrared (LWIR) imagery. In addition to the LUCINT12 two Nikon 850 camera were mounted on the aircraft. One Nikon collecting RGB and the other GBIR (green, blue and infrared > 715nm). The GBIR camera

produced false color infrared (CIR) images. The two camera systems operated independently though both systems used a GPS receiver to trigger the cameras to achieve a 75% overlap. The Nikon cameras stored RAW images to internal flash drives. The LUCINT12 cameras had internal hard drives and computer processors that immediately started to process the imagery into a single multi-layer tif from the different spectrums of the camera array.

To fly these systems on the fixed-wing aircraft, flight lines were created according to specified spatial extents and resolutions using both Aviatrix and LUCINT12 software. For the 2019 acquisition, there were 46 flight lines, at 80 knots, flown at 1780 ft above ground level (AGL). For the 2021 acquisition, there were 18 flight lines at 80 knots, flown at 2000 ft AGL. Maintaining consistent AGL was crucial for consistent resolution and imagery across varying topography. For the Nikon system, flight lines were built or loaded into Aviatrix Systems where the trigger time could also be selected. In the LUCINT12 system, simple polygons encompassing the flight area were uploaded with trigger times: once the aircraft entered the geographic location of the polygon, the cameras were activated and began collecting imagery. While cameras could be triggered based upon distance, I found that establishing consistent time intervals was more reliable overall. Regardless of the camera system used, the pilot was provided with the Aviatrix flight lines that included fixed resolution, height, and speed. Additionally, auto-exposure was completed before image collection and maintained for the duration of the flight. Camera operation tests were performed prior to or in flight to ensure that images were being taken and GPS correspondence was occurring.

During flights, all camera positions were recorded using a Trimble R7 GNSS rover (Trimble Navigation Unlimited, Sunnyvale, CA) with a NAD83 (2011) datum projection. Positioning error across images was less than 5 cm on average. All images were recorded in 14bit RAW (NEF) files, which were subsequently converted to 8-bit JPEG files using Adobe

Lightroom software (Adobe, Inc., San Jose, CA). Agisoft Metashape (Agisoft LLC, St. Petersburg, Russia) was then used for photogrammetric processing of the digital JPEG images. First, aerial control points were added and initial alignment reference settings were determined (*e.g.*, reporting camera accuracies and selecting accuracy requirements). Once an initial alignment was performed, optimization was conducted to improve alignment. This involved cleaning by removing outliers to re-optimize and reduce reconstruction uncertainty. This process of cleaning and optimizing was repeated until alignment distortion was sufficiently minimized. I then created digital elevation models (DEMs) from the processed sparse and dense clouds. I used only the sparse cloud to build the orthomosaic images. Although the DEM from the dense cloud was not necessary for building the orthomosaic, it may be useful for future studies with higher spatial resolution. Finally, I performed color calibration on both orthomosaics in order to even out the overall exposure and color variance. Spatial resolution for the 2019 imagery was 0.1 m (10 cm) and 0.05 m (5 cm) for the 2021 imagery. All imagery and spatial data points were projected into NAD83(2011) UTM zone 5N.

#### *Aerial orthoimagery classification*

Both the 2019 and 2020 imagery were exported into tiles and mosaiced together using ArcGIS Pro (ESRI Inc., Redlands, CA, United States). From the resulting orthomosaics, I created a training data set consisting of points assigned to three of the dominant land cover classes represented across the grassland: tree, shrub, and grass. I also included snow as a land cover class in the 2019 classification in order to prevent potential classification errors. Snow was not present in the 2021 imagery.

I sought to create training data for each class that reflected the range of spectral variability represented across each class (*e.g.*, selecting training data for the tree class that

corresponded with both overexposed or light-colored trees and trees with dark foliage). The training data was then imported into the “Create Signature File” tool in ArcGIS Pro to assign corresponding spectral data values to each class. I then used the “Maximum Likelihood Classification” tool to classify the imagery. In some portions of the classified imagery, I observed some speckling due to misclassified pixels. Because misclassified pixels were generally isolated and surrounded by correctly classified pixels, I applied an aggregation function in ArcGIS Pro to the 2021 classification using a cell factor of 6 and the “maximum’ aggregation technique in an effort to minimize the salt-and-pepper effect. For the 2019 classification, the aggregation was performed with a cell factor of 2 rather than 6 since the classification was less affected by speckling. As a result, spatial resolution for the 2019 classification 0.3 m (30 cm) and 0.2 m (20 cm) for the 2021 classification.

Lastly, variable cloud cover present during the 2021 image acquisition caused differences in exposure that made consistent classifications across the imagery difficult. To minimize spectral differences owing to variable exposure, I divided the imagery into five separate tiles of similar exposure, classified each tile individually, and then mosaiced the tiles together to recreate the full orthomosaic. Variability in exposure was less prevalent in the 2019 imagery; accordingly, I was able to classify the imagery using only two larger tiles.

#### *Ground-truth data collection*

During summer 2021, I conducted field surveys across Caribou Hills to validate the location and number of trees on the ground. While ground data is often used as both training and validation data for supervised classifications, I only used the ground data to validate the classifications, as the large spatial extent of the study area, in combination with time and access restrictions, limited the amount of data that would otherwise be necessary. Due to the limited



accessibility across the Caribou Hills grassland, I collected ground-truth data from plots (n=25) spaced roughly 200 m apart along an ATV trail that spanned the boundary of the 2021 imagery. This sampling design allowed me to account for spatial variability across the study area. At each plot, I collected the location of the plot center using a Trimble rover and remote. By communicating with local base stations, the location recorded by the rover was estimated to be accurate within a couple millimeters. I then counted and measured all spruce trees that occurred within a 10 m radius of the plot center (Fig. 6a). For each tree, metrics included: species; height (m); diameter at breast height (DBH, inches); estimated tree canopy radius (cm); distance from plot center (m); and bearing from plot center (degrees; Fig 6c). To assist with visualization of individual tree locations within the plots, I also recorded their locations on a cardinal birds-eye view graph. Lastly, I took a photograph in each cardinal direction from the plot center (Fig. 6d). If live spruce trees were not present in the plot, I recorded dead spruce, as they are visible in the aerial imagery and could still be used as validation data. After plot 25, the trail was no longer passable. The downloaded spatial location data was processed using GrafNav post-processing software (NovAtel Inc.) and time stamp logs were investigated to differentially correct the GNSS coordinates accordingly. This produced a table of coordinates in latitude and longitude to be used later for downstream accuracy assessments.

### *Classification accuracy assessments*

To assess the performance of the land cover classification models, I calculated a series of Confusion matrices using two separate independently-derived sets of validation data for which the true land cover classes values were known: (1) points created via on-screen digitization of high-resolution aerial imagery; and (2) ground-truth field data collection points.

To build validation data from the high-resolution aerial imagery, I created a gridded fishnet across the imagery and created one point for each class (tree, shrub, grass) within each grid block. I used this sampling design in order to create a systematic sample of the imagery and provide an equal representation of each land cover class, regardless of its abundance across the image. In the 2019 imagery, I created 85 validation points for each class from a 5x17 grid (n=85 grid polygons). In the 2021 imagery, 65 validation points were created from a 5x13 grid (n=65 grid polygons).

To create the ground-truth validation data, I used ArcGIS Pro to create a shapefile of plot centers from the GPS coordinates that I collected in the field. Next, I created 10-meter buffers around each plot center point to depict the size of each plot on the classified image (Fig. 6a). The ground-truth data (tree species/number, distance from plot center, bearing, tree size [radius, DBH, height]) and corresponding photographs were then used to identify where in the imagery trees were present on the ground. If the trees recorded on the ground had a DBH less than 2 inches, then they were not selected in the imagery, as these trees were generally too small to observe in the imagery given the spatial-resolution. All other trees recorded on the ground were identified and marked as belonging to the “tree” class across 23 plots and both sets of imagery (n=90). Grass and shrub points were not recorded on the ground; therefore, I selected 90 points per class as evenly as possible across the 23 plots using the aerial imagery and ground photographs as a reference.

For each set of validation points, I extracted the pixel values (*i.e.*, land cover class) from the classified orthomosaic and computed a confusion matrix between the values assigned to the validation points and the classified values in ArcGIS Pro. To estimate the classification accuracy of the 2019 and 2021 imagery, I calculated total overall classification accuracy, as well as Producer’s Accuracy and User’s Accuracy for each class. Producer’s accuracy was calculated by

dividing the number of correctly classified pixels, along the matrix diagonal, assigned to a category by the total number of reference pixels that were classified in that class (*i.e.*, error of omission). This metric indicates the level to which the reference points have been accurately mapped. User's accuracy, on the other hand, was calculated by dividing the number of correctly classified pixels in each class by the total number of pixels that were classified in that class (*i.e.*, error of commission). It indicates the probability that a pixel assigned to a particular class actually represents that same class on the ground (Petersen et al., 2005; Congalton, 1991). To compute Producer's Accuracy and User's Accuracy, the confusion matrix lists the number of data points associated with each class and then calculates how that pixel compares to the ground data, as well as how it compares to other classes.

## RESULTS

### *Land cover classification accuracy*

Using a supervised Maximum Likelihood Classification approach, I classified trees, shrubs, grass, and snow (where applicable) from aerial imagery collected in the Caribou Hills grassland in 2019 (Fig. 2) and 2021 (Fig. 3). This approach produced highly accurate land cover classifications across both years and across areas of differing vegetation composition and configuration, including in areas with fewer, more isolated trees (Fig. 4a), as well as in areas with high vegetative cover characterized by densely clumped trees and shrubs (Fig. 4b).

Overall, classification accuracies across both images were above 78% (Table 1 & 2). Differences in accuracy across a single image collection may be due to the restricted area of ground validation data compared to gridded based validation data, particularly in the case of the 2019 classification. Overall, the classification of the RGB imagery collected in 2019 produced a

higher gridded accuracy than that of the RGB imagery collected in 2021, using both gridded and ground-truth accuracy assessment methods. The highest overall accuracy obtained for the 2019 classification was 96.8% (kappa = 0.96; Table 1), whereas the highest overall accuracy obtained for the 2021 classification was 89.7% (kappa = 0.85; Table 2). When accuracy was assessed using the ground-truth validation data, the highest overall accuracy obtained for the 2019 classification was 78.6% (kappa = 0.712; Table 1), while the highest overall accuracy obtained for the 2021 classification was 89.0% (kappa = 0.83; Table 2).

User's and Producer's accuracies across both years were above 83%, with the exception of two cases (Table 1). In the 2019 classification gridded accuracy assessment, all User's and Producer's accuracies were above 89% (Table 1). In the 2021 classification ground-truth accuracy assessment, the lowest Producer's accuracy was 74.7% in the tree class (Table 2). The rest of both User's and Producer's accuracy were above 70%. In the 2021 classification gridded accuracy assessment, the lowest Producer's accuracy was 83.1% (Table 2). The rest of both User's and Producer's accuracy were above 83% (Table 2).

In the 2019 classification ground-truth accuracy assessment, the lowest User's accuracy was 59.6% in the grass class (error of commission; 90/151 grass classified points were groundtruthed as grass; Table 1). The lowest Producer's accuracy was 49.5% in the shrub class (error of omission; 47/95 ground-truthed shrub points were classified as shrub as opposed to another class or 48/95 were misclassified as other classes; Table 1).

#### *Accuracy assessment of aggregated vs. non-aggregated classifications*

To minimize the salt-and pepper effect that resulted from the classification of the high resolution (0.05 m) 2021 imagery, I applied an aggregation function to the 2021 land cover classification (Fig. 5). Overall accuracies (gridded or ground-truth) for the classification with the

aggregation function applied were lower than the classification without aggregation. The average overall accuracy for the classification with aggregation applied was 77.85% and 89.35% for the classification with no aggregation (Table 3). Additionally, Producer's accuracies for the tree class were lower in both gridded and ground-truth accuracy assessments of the aggregated classification at 67.7% and 51.6%, respectively, in comparison to the same classification without aggregation (Table 3). Producer's accuracies for the tree class in both gridded and ground-truth accuracies for the classification without aggregation were 84.6% and 74.7%, respectively (Table 3).

#### *Coverage of classified land cover classes*

The 2019 imagery covered an area of about 251 km<sup>2</sup> while the 2021 covered 38 km<sup>2</sup> (roughly 15% of the 2019 area (Fig. 1 and Fig. 2). Based on the 2019 classification of the RGB imagery, 3.13% (7.9 km<sup>2</sup>) of the image was classified as tree; 25.3% (63.5 km<sup>2</sup>) was classified as shrub; 67.4% (169.2 km<sup>2</sup>) was classified as grass; and 4.1% (10.3 km<sup>2</sup>) was classified as snow (Table 4). The 2021 classification with aggregation applied, had 2.75% (1 km<sup>2</sup>) of the area classified as tree cover; 29.6% (11.3 km<sup>2</sup>) classified as shrub; and 67.6% (25.7 km<sup>2</sup>) classified as grass (Table 4). In contrast, for the 2021 classification without aggregation, about 7.25% (2.75 km<sup>2</sup>) was classified as tree cover; 34.38% (13.1 km<sup>2</sup>) was classified as shrub; and 58.36% (22.2 km<sup>2</sup>) was classified as grass (Table 4). Based on these data, the difference in tree cover between the 2019 and 2021 (with aggregation) classifications was 0.38%; the difference in shrub cover was 4.3%; and the difference in grass cover was 0.2% (Table 4). The differences in percent cover between the 2019 and 2021 classifications were greater without aggregation: the difference in tree cover was 4.12%; the difference in shrub cover was 9.07%; and the difference in grass cover

was 9.07%. As there was no snow present in the 2021 imagery, I did not calculate change in the snow class between years.

## DISCUSSION

In this study, I used high-resolution aerial imagery to classify land cover across the Caribou Hills grassland region on the Kenai Peninsula of Alaska, USA following large-scale disturbance from SBB outbreak and wildfire events to provide preliminary insights regarding whether, or to what degree, this landscape may be shifting from a forested to a savannah-like ecosystem. By doing so, I sought to develop an accurate and efficient approach that could be used by land managers as a tool to monitor ecosystem shifts in this and other similarly dynamic landscapes into the future. I classified aerial imagery from two separate aerial acquisitions, each collected from a different time period within the growing season and each with varied spatial resolution, to evaluate how seasonality, size, and spatial grain influenced classification accuracy. I also assessed how classification accuracy varied in response to the use of different filtering and validation approaches.

### *Accuracy of land cover classifications*

I generated accurate predictions of land cover from aerial imagery collected in 2019 and 2021 across the Caribou Hills grassland on the Kenai Peninsula of Alaska. Using two separate approaches to assess classification accuracy, I obtained overall accuracies ranging from 89% to 97% (Table 1 & 2). Despite high overall accuracies, however, accuracies varied between the 2019 and 2021 aerial imagery land cover classifications, suggesting that seasonality and the spatial resolution of the imagery had an effect on the ability of the classification approach to distinguish between assigned land cover classes.

I found that the 2019 spring collection was visually cleaner with minimal speckling, and had slightly stronger accuracies. Because this acquisition was collected in the spring, before deciduous trees and shrubs had leafed out, the tree and shrub classes appeared very distinct from the surrounding matrix of grass. In contrast, the land cover classes appeared less distinct from one another in the August 2021 image collection, with trees, shrubs, and grass exhibiting relatively similar spectral characteristics in the visible range. The goal behind the Summer 2021 collection was to equip cameras with a sensor to capture IR, in addition to RGB, in order to obtain a stronger ability to distinguish between the three landcover classes. However, the addition of the IR band in the summer acquisition did not contribute to delineation as much as expected. Extracting and performing the classification with just the IR band would be worth testing in the future for both delineation purposes, as well as for additional classification objectives. Lastly, while a summer acquisition may be more useful for identifying biodiversity or species delineation, the spring acquisition (prior to leaf-out) proved more effective for land cover classification in this region.

#### *Effect of spatial aggregation on classification accuracy*

While the classification of the summer 2021 imagery did characterize trees and shrubs well, many small, isolated grass pixels were misclassified as trees causing more speckling as a result of greater similarity in natural color compared to the spring imagery collection. Given that the majority of these misclassified pixels were isolated and surrounded by accurately-classified pixels, I used the “Aggregate” tool in ArcGIS Pro to resample the classified image to a coarser resolution using the ‘maximum’ technique with a cell factor of 6 (Fig. 5). The “Aggregate” tool takes the number of selected pixels (*i.e.*, cell factor of 6 as defined in this study), determines of the 6 pixels which class was most common, and assigns all 6 pixels that class. For example, if

there was one tree pixel surrounded by five grass pixels, the “Aggregate” tool would assign all six pixels to the grass class based on a “maximum” rule. While the tool worked well to eliminate most small discretions, there were several instances in which the tool created larger blocks of incorrectly classified pixels. Accordingly, I evaluated multiple cell factor values factors to determine which struck the best balance between these two components. For example, the nonaggregated 2021 classification captured the trees much better than the aggregated version, but the salt and pepper speckled effect was much more prevalent (Fig. 5). On the other hand, the aggregated version appeared cleaner with less speckling, but created larger misclassified blocks, which were especially noticeable within captured trees (Fig. 5). The non-aggregated classification also resulted in higher overall accuracies but because of the salt and pepper effect, the incorrectly classified pixels spread among the grass class likely resulted in less accurate percent cover values (Table 3 & 4), where the percent cover values are likely over-estimated for trees and underestimated for grass. On the other hand, the percent cover values among the aggregated classification (where there was less speckling present), are likely to be more accurate overall but potentially under-estimated the tree class percent cover value. I used the “Aggregate” tool for the 2019 imagery but with a much smaller cell factor of 2 as it had minimal salt and pepper effect. While acquisition of aerial imagery during the summer may be preferable when the goal is to monitor biodiversity, spring imagery acquisitions are more likely to generate classifications of higher accuracy owing to the greater ability to delineate between vegetation cover types before leaf out.

#### *Ground-truthed vs. image-based validation approaches*

As expected, I found that the method by which I derived validation data – whether via ground-truthed data collection or via an independently-derived systematic sample of the original



imagery (“gridded method”) – influenced my resulting estimates of classification accuracy. Because accessibility in the Caribou Hills was restricted to public land, as well as to areas accessible via ATV and foot, I was only able to collect ground validation data from along a single trail spanning in the East-West direction across the grassland. While I attempted to capture as much variation in my ground-truthed samples as possible, the ground-truthed validation data was relatively clumped and limited to a smaller spatial extent that did not include the geographic spread, spectral quality and spectral diversity across the landscape as compared to the validation data that I created by using the gridded method. The gridded method contained validation points derived from nearly 70 locations or “plots” across the landscape; validation points collected on the ground came from 20 plots distributed across a smaller area. Furthermore, to ensure that data collection was feasible and practical, plot sizes were limited to a 10 m radius and contained more clumped trees, which I found to be more difficult to distinguish from one another in the classifications.

The ground data-based 2019 classification accuracy assessment was notably lower than the gridded assessment in 2019. The overall accuracy for the 2019 gridded assessment was 96.8% while the accuracy for the 2019 ground-truth assessment was 78.6% (Table 1). The ground-truth plots traverse a portion of the imagery with particularly low exposure (Fig.1). It is possible that the quality of classification was poorer in this region due to the low exposure, rendering lower accuracies. Additionally, the ratio between the area the ground data covered to the entire region is much smaller in the 2019 imagery in comparison to the 2021 imagery. The ground data is not as strong as a representative dataset for validating the 2019 classification. In the 2021 classification, the difference between the ground-data assessment and the gridded assessment was not as striking as it was in 2019. The overall accuracy for the 2021 gridded assessment was 89.7% while the accuracy for the 2021 ground-truth assessment was 89.0%

(Table 2). In this case, the ground plots traversed a portion of the imagery that was situated within one of the five tiles, signifying that exposure was a bit more consistent across this area compared to 2019 which crossed both tiles with high variation in exposure.

Although estimates of classification accuracy were lower when I used the ground-truthed data to validate the classifications (Table 1 & 2), ground-truthed data provided less biased data, as trees, shrubs and grass were visually accounted for on the ground. This contrasts the gridded method validation, where each class was identified visually in the original imagery, but not identified on the ground. Accordingly, future image classification efforts should consider both validation methods in order to account for the benefits and limitations associated with each when performing classification accuracy assessments.

In the future, several considerations should be taken into account when collecting ground validation data that may improve their use. First, although recording the GPS location of only a single point at the center of the plot and then identifying the number and approximate location of each tree within the plot was efficient, this method necessitated discretion to confidently match trees marked on the ground to their respective counterparts in the imagery. To avoid this discretion in the future, I recommend instead marking individual trees with a survey-grade GPS unit and recording its associated attribute data. Second, I recommend selecting plots with trees spaced further apart, or without overlapping canopies, as opposed to plots with trees in more clumped configurations in order to make it easier to match trees on the ground to trees in the corresponding imagery. While I dictated that ground-truthed trees needed to have a DBH of 2 inches to adequately account for the spruce seen on the ground and in both sets of imagery, some spruce as small as 1.5 inch DBH, 2 meter height, and 40-50 cm radius were visible in both sets of imagery. The 2021 classification, which had a higher spatial resolution performed better in capturing smaller individual spruce trees, whereas the 2019 classification rarely captured spruce

with DBH under 2 inches. Lastly, depending on research objectives, it may be important to collect attributes of each tree on the ground, such as height, radius and DBH; however, in the case of this study, tree radius was the most useful metric for illustrating the ground data.

#### *Implications of land cover class composition*

The percent cover values were calculated using the total pixel number for each class divided by total number of pixels. As seen in both 2019 and 2021 classifications, grass has the highest percent cover, followed by shrub and then tree, which had the lowest percent cover. Given that this region was historically considered to be a spruce-dominated forest, as recent as the 1990s, this shift to a landscape dominated by grass is a significant point to consider (Hess et al., 2019). While what classifies a grassland is vague and precedent, Dixon et al. 2014 in their study on global grassland types highlights some defining characteristics based around the International Vegetation Classification (IVC), and Terrestrial Ecoregions of the World (TEOW): stating that, “Grass dominance is expressed when graminoids have over 25% grass cover (Kucera, 1981); Shrub cover in grasslands is typically less than 25%; and trees in temperate zones, typically have less than 10% canopy cover, are over 5 m tall and single-layered; Single dry season over 4 months; Fires regular; often in sites with seasonal waterlogging; Shrublands can be defined where shrubs are over 0.5 m tall and have over 25% shrub cover; and tree cover is less than 10%.” Accordingly, if the Caribou Hills region, which was classified as being composed of 67.54% grass on average (between 2019 and 2021 classifications), was to be defined based on the aforementioned characteristics, it would imply strong grass dominance (Table 4). However, because shrub coverage was estimated to comprise 27.46% on average, of the landscape, this suggests that this landscape may alternatively be considered a shrubland

under the IVC designation (Table 4). Lastly, tree coverage was estimated to be below 10% canopy cover, at about 2.94% on average (Table 4).

While these definitions are useful in identifying whether or what kind of grassland this landscape falls under, these acquisitions are only a snapshot in time. Warm, dry summer seasons are becoming longer and more extreme (Wendler et al., 2009; Hinzman et al., 2005). These trends, along with anthropogenic factors, are increasing wildfire risk and the fire season length in this region. This raises questions surrounding how effective prior grassland definitions are in studying or managing increasingly dynamic landscapes. A study surrounding global grassland types, emphasized the diversity in grassland landscapes, identifying 49 taxonomically and spatially distinct grassland types (Dixon et al., 2014). With high anthropogenic influence, whether development or climate-based, grasslands span from human-made grass pastures to large-scale ecosystems that could be a fusion of grassland, a shrubland or late succession forest (FAO, 2005; Dixon et al., 2014). Landscapes such as the Caribou Hills are therefore forcing managers to rethink management strategies and question if stewardship may offer more biodiversity or flourishing than conservation of preceding or familiar landscapes. New definitions should be considered that allow for greater flexibility in grassland ecosystems in order to better manage and study grassland or other ecosystem conversions (Dixon et al., 2014).

The estimated percentages of each land cover class, when considered across classifications of both 2019 and 2021 years, offer additional interesting insights into the dynamics occurring in the Caribou Hills region. Considering the recent disturbance history of the Caribou Hills, a shrub cover of 27.46% on average, is quite high, suggesting possible shrubification. Shrubbyfication is the process of shrub expansion across Boreal and Arctic systems (Mekonnen et al., 2021). Shrub expansion has been shown to be a response to climate warming

and may drive changes in competitive interactions, altering landscape composition, ecosystem structure, function, feedbacks, fire, animal habitat and subsistence practices (Mekonnen et al., 2021; Forbes et al 2010; Cornelissen et al 2001; Elmendorf et al 2012; Loranty and Goetz 2012; Camac et al 2017; Tape et al 2016; Henry et al 2012). Although shrubification has been found to be a more common phenomenon in northern Alaska (Mekonnen et al., 2021), it has been recently recorded in south-central Boreal and coastal ecosystems (Berg et al., 2009; Boucher et al., 2006)

Similar to how shrubs are showing perseverance in regions experiencing intense climatic changes, graminoid species are also competitive in dry, warm areas due to their ability to perform C4 photosynthesis. C4 grasses evolved with seasonal climatic aridification or atmospheric change and typically grow in exclusively open terrestrial areas (Dixon et al 2014). The Boreal region is seeing dramatic atmospheric change and climatic aridification that, in combination with large effects from disturbance, provide grasses and shrubs greater competitive ability over slow-recruiting species such as spruce. Once established, grasses have a much shorter fire regime than that of a spruce forest. The Caribou Hills has historically been characterized as having a 400–600-year fire regime (Berg & Anderson, 2006); recently, the region is experiencing annual spring fires and land managers have already demanded that the local fire department expand its fire season as a result of changing ecosystems (Alaska Interagency Coordination Center, 2010). This reduced length of the historical fire regime is predicted to further perpetuate slow or non-existent forest succession, while promoting grass dominance.

When considered across the two years of aerial imagery classifications, I found slight changes associated with percent coverages of each land cover type. For example, tree coverage declined by 0.38% between 2019 and 2021 (with aggregation), shrub coverage increased by 4.3% and grass coverage remained relatively stable (67.43% to 67.65% from 2019 to 2021; Table

4). This compositional distribution may be explained by spruce recruitment being suppressed by competition from grasses and shrubs. The dominant species of grass in the Caribou Hills Grassland region is *Calamagrostis canadensis*, commonly known as Bluejoint Reedgrass (Tracy Melvin, *personal communication*). While this species is native, it is an aggressive repopulator that thrives and disperses rapidly in post-disturbance landscapes. It builds a thick root mat at the surface of the soil, often preventing other species from establishing. Previous studies have shown that seedling abundance was significantly lower in plots with over 60% bluejoint litter coverage, yet significantly greater in plots with bluejoint litter below 60%, indicating a threshold of bluejoint grass in restricting seedling establishment (Boggs et al., 2008). While it may be geographically dependent, grass did cover over 60% of this landscape in both 2019 and 2021 classifications (Table 4): this indicates that a threshold may have been exceeded, potentially explaining slow and minimal spruce recruitment across the region. The Caribou Hills Grassland ecosystem also currently lacks a foundation species. During the Pleistocene, when the climate was arid and the Caribou Hills were grassy, steppe-bison initiated nutrient recycling and grazed on dominant grasses. While there are a few small herds of caribou in this region, there is not a large enough grazer presence to keep a grassland of this scale in balance. Nonetheless, the observed increase in shrub coverage by almost 5% may be indicative of successful and rapid establishment in the grassland. Comparing changes in the overall coverages of each land cover class over time will provide managers with a better understanding of the ecological trajectory of the Caribou Hills, in turn offering valuable insights into its management.

However, in this study, it is important to note that the two years of classified imagery may not be directly comparable, as the imagery was collected at two different times of year, using two different camera systems, and encompassing two separate areas of varied spatial extent. For example, the 2019 land cover classification represented a much larger spatial extent

than that in 2021. Nonetheless, in spite of differences in image acquisition extents, the percent coverage values of each land cover class were very similar between the two classifications. Given the challenges associated with collecting and processing aerial imagery (*e.g.*, cost and time) for the entire Caribou Hills region, which spans approximately 251 km<sup>2</sup>, the observed similarities between the two classifications indicates that image acquisition and ground-truth validation from smaller spatial extents, such as that conducted in 2021, may serve as a useful proxy for the Caribou Hills region as a whole, provided that the area captures sufficient variation across the land cover classes. In turn, the classifications and methodology presented here provide a valuable framework for assessing changes in vegetation cover over time or to model ecosystem shifts.

#### *Recommendations for aerial imagery classification efforts*

Both land cover classifications were highly accurate and offer significant insight into what is known about land cover in this region. However, there are several considerations that should be taken into account that could further improve classifications of aerial imagery in the future. First, as mentioned previously, processing the 2019 imagery, which covered a very large spatial extent took a very long time and required significant processing power. Accordingly, acquiring imagery over a smaller area representative of the grassland overall would serve as a useful proxy and would enable managers to process images more efficiently and with similar accuracy. Alternatively, imagery could be divided into tiles and processed individually before mosaiced back together. This would help eliminate some exposure implications.

Second, aerial imagery should ideally be collected on a clear or overcast day. Due to variable cloud cover in the 2021 acquisition, differences in exposure across the acquisition area resulted in spectral differences across the image that made classification of the full spatial extent

difficult. It was likely for this reason that the classification gridded accuracy was lower for the 2021 classification compared to the 2019 classification gridded accuracy (Table 1 & 2). In an effort to reduce the effect of spectral confusion between land cover classes due to differences in exposure across the image, I divided the orthomosaic into several tiles of smaller extent and that minimized variability in exposure in each. I then classified each tile individually and finally mosaiced the tiles back together to recreate the full classified orthomosaic. The 2019 imagery was split into two tiles based on exposure, while the 2021 imagery was split into five tiles based on exposure. Doing this enhanced the overall quality and cohesiveness of the classification. Differences in classification as a result of exposure can be seen in Fig. 7; there is a distinct line that highlights how grass is incorrectly classified as shrub below but correctly classified as grass above it. Which class was chosen was dependent on the exposure of the tile it was contained within. Ideally, exposure would be consistent across the entire study area but cloud movement caused exposure to differ even within a single flight line. While tiling the study area into areas of similar exposure enhanced the overall quality and cohesiveness of the classifications, variability in exposure within a single tile still impacted classification accuracy.

Lastly, while the maximum likelihood classification method used in this study was successful and replicable; numerous other approaches exist to classify aerial imagery, including image segmentation (using the “Mean Shift” tool), object-based classification, creating training data with polygons as opposed to points, or using a convolution filter. Different classification methods should be considered depending on the research objectives of a given study.

Additionally, other related classification objectives could be studied with remote sensing or aerial imagery. For example, aerial imagery can be used to measure biodiversity. Because species reflect different amounts of infrared light back into the atmosphere, infrared aerial imagery can



be used to identify between species types and abundance. If infrared imagery is not feasible, NDVI can be calculated from near-infrared and RGB bands for a similar effect.

Classification using IR or NDVI would be useful in measuring and monitoring biodiversity on a larger scale or in more remote areas where field work methods are not able to be performed.

However, the workflow in this study may offer complementary insights when the objective is to classify broad vegetation types across the landscape.

### *Future directions*

The classification method presented in this study aided in identifying the composition of the Caribou Hills Grassland and has implications for monitoring vegetation change over time.

The Caribou Hills Grassland has experienced a significant and rapid ecosystem shift over the last several decades, transitioning from a historically spruce-dominated forest to what is now primarily a grassland with less than 5% tree cover. Nevertheless, as the SBB outbreak and wildfires were relatively recent, there is potential for forest succession to occur slowly yet steadily over time. Using the approach developed in this study to classify major vegetation types in the grassland will be important for monitoring the future of the region as a whole. In addition to monitoring the potential ecosystem shift from forest to grassland, this method may be extended to monitor other processes including shrubification, spruce recruitment, and disturbances.

Furthermore, it may be of interest to classify spruce trees as points across the grassland to perform point-pattern analyses. Point-pattern analyses could provide valuable insight into the recruitment and succession of spruce which will largely dictate the ecology of the region and future biodiversity. Consistent work flows to classify individual spruce trees as points is

currently still in development, but will provide valuable information to enhance our collective understanding of spruce recruitment within the grassland.

Using remote sensing and classification methods similar to those in this study should be taken advantage of across other regions of the Arctic, or globally to monitor and understand large-scale and/or remote landscape change. The ways in which aerial imagery and classification methods can be used is expanding and constantly being explored. This study focused on one of these ways but with larger aims to encourage further use of remote sensing and GIS approaches.

However, it is imperative to consider the challenges associated with using remote sensing technology for monitoring. Managers and remote sensing scientists must work together as both fields are specialized in method and ideology (Kennedy et al., 2009). Remote sensing scientists must understand the needs and approach of the managers' goals, and the managers must have or develop an understanding of the fundamental remote sensing issues that arise in detection and monitoring projects (Kennedy et al., 2009). Remote sensing technology is still being built and tested, which contributes to present restrictions. It can take decades to acquire and develop a reliable system that encompasses a diversity in acquisitions. Education, training and experience will be key in sharing remote sensing knowledge across disciplines

### *Conclusion*

By developing an approach to delineate land cover in a dynamic landscape such as the Caribou Hills grassland – an area that has experienced significant impacts from SBB outbreak, wildfire, and drought conditions in the past three decades – this study provides a strong foundation for future research and monitoring. Furthermore, while monitoring patterns of recruitment, succession, and biodiversity will be incredibly valuable for adaptive management in the Caribou Hills grassland region, the workflow developed in this study is flexible and may

serve as a useful framework for remote monitoring of other regions experiencing similar ecological or climatic shifts.

## REFERENCES

Alaska Interagency Coordination Center, Alaska Interagency Wildland Fire Management Plan 2010 (2010). Fort Wainwright.

Wendler, G., & Shulski, M. (2009). A Century of Climate Change for Fairbanks, Alaska. In *Source: Arctic* (Vol. 62, Issue 3).

Baughman, C. A., Loehman, R. A., Magness, D. R., Saperstein, L. B., & Sherriff, R. L. (2020). Four decades of land-cover change on the Kenai Peninsula, Alaska: Detecting disturbance-influenced vegetation shifts using landsat legacy data. *Land*, 9(10), 1–22.  
<https://doi.org/10.3390/land9100382>

BEA, 2018: Alaska: Personal income. Bureau of Economic Analysis Rep., 3 pp.,  
<https://apps.bea.gov/regional/bearfacts/pdf.cfm?fips=02000&areatype=02000&geotype=3>.

Berg, E. E., & Anderson, R. S. (2006). Fire history of white and Lutz spruce forests on the Kenai Peninsula, Alaska, over the last two millennia as determined from soil charcoal. *Forest Ecology and Management*, 227(3 SPEC. ISS.), 275–283.  
<https://doi.org/10.1016/j.foreco.2006.02.042>

Berg, E. E., David Henry, J., Fastie, C. L., de Volder, A. D., & Matsuoka, S. M. (2006). Spruce beetle outbreaks on the Kenai Peninsula, Alaska, and Kluane National Park and Reserve, Yukon Territory: Relationship to summer temperatures and regional differences in disturbance regimes. *Forest Ecology and Management*, 227(3 SPEC. ISS.), 219–232.  
<https://doi.org/10.1016/j.foreco.2006.02.038>

- Berg, E.E.; Hillman, K.M.; Dial, R.; DeRuwe, A. Recent woody invasion of wetlands on the Kenai Peninsula Lowlands, south-central Alaska: A major regime shift after 18 000 years of wet Sphagnum–sedge peat recruitment. *Can. J. Res.* 2009, 39, 2033–2046.  
<https://doi.org/10.1139/X09-121>
- Berman, M., Schmidt, J. I., & Berman, M. (n.d.). *REVIEW Economic Effects of Climate Change in Alaska*. <https://doi.org/10.1175/WCAS-D-18-0056.s1>
- Bernhardt, J. R., & Leslie, H. M. (2013). Resilience to climate change in coastal marine ecosystems. *Annual Review of Marine Science*, 5, 371–392.  
<https://doi.org/10.1146/annurev-marine-121211-172411>
- Boggs, K., Sturdy, M., Rinella, D. J., & Rinella, M. J. (2008). White spruce regeneration following a major spruce beetle outbreak in forests on the Kenai Peninsula, Alaska. *Forest Ecology and Management*, 255(10), 3571–3579.
- Bonan, G. B. (n.d.). *Forests and Climate Change: Forcings, Feedbacks, and the Climate Benefits of Forests*. <https://www.science.org>
- Boucher, T.V.; Mead, B.R. Vegetation change and forest regeneration on the Kenai Peninsula, Alaska following a spruce beetle outbreak, 1987–2000. *Ecol. Manag.* 2006, 227, 233–246.  
<https://doi.org/10.1016/j.foreco.2006.02.051>
- Box, J. E., Colgan, W. T., Christensen, T. R., Schmidt, N. M., Lund, M., Parmentier, F. J. W., Brown, R., Bhatt, U. S., Euskirchen, E. S., Romanovsky, V. E., Walsh, J. E., Overland, J. E., Wang, M., Corell, R. W., Meier, W. N., Wouters, B., Mernild, S., Mård, J., Pawlak, J., & Olsen, M. S. (2019). Key indicators of Arctic climate change: 1971–2017. In *Environmental Research Letters* (Vol. 14, Issue 4). Institute of Physics Publishing.  
<https://doi.org/10.1088/1748-9326/aafc1b>

- Bradshaw, C. J. A., & Warkentin, I. G. (2015). Global estimates of Boreal forest carbon stocks and flux. *Global and Planetary Change*, *128*, 24–30.  
<https://doi.org/10.1016/j.gloplacha.2015.02.004>
- Buma, B. (2015). Disturbance interactions: Characterization, prediction, and the potential for cascading effects. *Ecosphere*, *6*(4), 1–15. <https://doi.org/10.1890/ES15-00058.1>
- Camac J S, Williams R J, Wahren C-H, Hoffmann A A and Vesk P A 2017 Climatic warming strengthens a positive feedback between alpine shrubs and fire. *Glob. Change Biol.* *23*:249–58. <https://doi.org/10.1111/gcb.13614>
- Carpenter, S., Walker, B., Anderies, J. M., & Abel, N. (2001). From Metaphor to Measurement: Resilience of What to What? *Ecosystems*, *4*(8), 765–781.  
<https://doi.org/10.1007/s10021-001-0045-9>
- Chapin, F. S., & Starfield, A. M. (n.d.). *TIME LAGS AND NOVEL ECOSYSTEMS IN RESPONSE TO TRANSIENT CLIMATIC CHANGE IN ARCTIC ALASKA.*
- Cohen, W. B., Healey, S. P., Goward, S., Moisen, G. G., Masek, J. G., Kennedy, R. E., Powell, S. L., Huang, C., Thomas, N., Schleeweis, K., & Wulder, M. A. (2007). *USE OF LANDSAT-BASED MONITORING OF FOREST CHANGE TO SAMPLE AND ASSESS THE ROLE OF DISTURBANCE AND REGROWTH IN THE CARBON CYCLE AT CONTINENTAL SCALES.*
- Congalton, R. G. (1991). *A Review of Assessing the Accuracy of Classifications of Remotely Sensed Data* (Vol. 37).
- Cornelissen J H C, Callaghan T V, Alatalo J M, Michelsen A, Graglia E, Hartley A E, Hik D S, Hobbie S E, Press M C and Robinson C H 2001 Global change and Arctic ecosystems: is

- lichen decline a function of increases in vascular plant biomass? *J. Ecol.* 89:984–94.  
<https://doi.org/10.1111/j.1365-2745.2001.00625.x>
- Côté, I. M., & Darling, E. S. (2010). Rethinking ecosystem resilience in the face of climate change. *PLoS Biology*, 8(7). <https://doi.org/10.1371/journal.pbio.1000438>
- Dial, R. J., Berg, E. E., Timm, K., McMahon, A., & Geck, J. (2007). Changes in the alpine forest-tundra ecotone commensurate with recent warming in southcentral Alaska: Evidence from Orthophotos and field plots. *Journal of Geophysical Research: Biogeosciences*, 112(4). <https://doi.org/10.1029/2007JG000453>
- Dixon, A. P., Faber-Langendoen, D., Josse, C., Morrison, J., & Loucks, C. J. (2014). Distribution mapping of world grassland types. *Journal of Biogeography*, 41(11), 2003–2019.  
<https://doi.org/10.1111/jbi.12381>
- Elmendorf S C et al 2012a Global assessment of experimental climate warming on tundra vegetation: heterogeneity over space and time *Ecol. Lett.* 15:164–75.  
<https://doi.org/10.1111/j.1461-0248.2011.01716.x>
- FAO (2010) Global forest resources assessment. Food and Agriculture Organization of the United Nations (FAO), Rome.
- Forbes B C, Fauria M M and Zetterberg P 2010 Russian Arctic warming and ‘greening’ are closely tracked by tundra shrub willows. *Glob. Change Biol.* 16:1542–54.  
<https://doi.org/10.1111/j.1365-2486.2009.02047.x>
- Goldsmith, S., 2010: Structural analysis of the Alaska economy: What are the drivers? Institute of Social and Economic Research, University of Alaska Anchorage Rep., 144 pp., <https://scholarworks.alaska.edu/handle/11122/4287>.

- Gonzalez, P., Neilson, R. P., Lenihan, J. M., & Drapek, R. J. (2010). Global patterns in the vulnerability of ecosystems to vegetation shifts due to climate change. *Global Ecology and Biogeography*, 19(6), 755–768. <https://doi.org/10.1111/j.1466-8238.2010.00558.x>
- Grimm, N. B., Chapin, F. S., Bierwagen, B., Gonzalez, P., Groffman, P. M., Luo, Y., Melton, F., Nadelhoffer, K., Pairis, A., Raymond, P. A., Schimel, J., & Williamson, C. E. (2013). The impacts of climate change on ecosystem structure and function. In *Frontiers in Ecology and the Environment* (Vol. 11, Issue 9, pp. 474–482). <https://doi.org/10.1890/120282>
- Hansen M. C., Potapov Peter, Moore R., Hancher M., Turubanova Svetlana, Tyukavina Alexandra, Thau D., Stehman Stephen, Goetz Scott, Loveland Thomas, Kommareddy Anil, Egorov Alexey, Chini L., Justice C. O., and Townshend J.. 2013. High-Resolution global maps of 21st-century forest cover change. *Science* 342, 6160 (2013), 850–853. <https://doi/10.1126/science.1244693>
- Hansen, W. D., Chapin, F. S., Naughton, H. T., Rupp, T. S., & Verbyla, D. (2016). Forest landscape structure mediates effects of a spruce bark beetle (*Dendroctonus rufipennis*) outbreak on subsequent likelihood of burning in Alaskan Boreal forest. *Forest Ecology and Management*, 369, 38–46. <https://doi.org/10.1016/j.foreco.2016.03.036>
- Hayes, D. J., McGuire, A. D., Kicklighter, D. W., Gurney, K. R., Burnside, T. J., & Melillo, J. M. (2011). Is the northern high-latitude land-based CO<sub>2</sub> sink weakening? *Global Biogeochemical Cycles*, 25(3). <https://doi.org/10.1029/2010GB003813>
- Henry G H R, Harper K A, Chen W, Deslippe J R, Grant R F, Lafleur P M, Lévesque E, Siciliano S D and Simard S W 2012 Effects of observed and experimental climate change on terrestrial ecosystems in northern Canada: results from the Canadian IPY program *Clim.*



Change 115207–34. <https://doi.org/10.1007/s10584-012-0587-1>

Hess, K. A., Cullen, C., Cobian-Iñiguez, J., Ramthun, J. S., Lenske, V., Magness, D. R., Bolten, J. D., Foster, A. C., & Spruce, J. (2019). Satellite-based assessment of grassland conversion and related fire disturbance in the Kenai Peninsula, Alaska. *Remote Sensing*, *11*(3). <https://doi.org/10.3390/rs11030283>

Hinzman, L. D., Bettez, N. D., Bolton, W. R., Chapin, F. S., Dyrurgerov, M. B., Fastie, C. L., Griffith, B., Hollister, R. D., Hope, A., Huntington, H. P., Jensen, A. M., Jia, G. J., Jorgenson, T., Kane, D. L., Klein, D. R., Kofinas, G., Lynch, A. H., Lloyd, A. H., McGuire, A. D., ... Yoshikawa, K. (2005). Evidence and implications of recent climate change in Northern Alaska and other Arctic regions. *Climatic Change*, *72*(3), 251–298. <https://doi.org/10.1007/s10584-005-5352-2>

Iverson, L. R., Graham, R. L., & Cook, E. A. (1989). Applications of satellite remote sensing to forested ecosystems. In *Landscape Ecology* (Vol. 3, Issue 2). SPB Academic Publishing

Kennedy, R. E., Townsend, P. A., Gross, J. E., Cohen, W. B., Bolstad, P., Wang, Y. Q., & Adams, P. (2009). Remote sensing change detection tools for natural resource managers: Understanding concepts and tradeoffs in the design of landscape monitoring projects. *Remote Sensing of Environment*, *113*(7), 1382–1396.

<https://doi.org/10.1016/j.rse.2008.07.018>

Kerr, J. T., & Ostrovsky, M. (2003). From space to species: Ecological applications for remote sensing. In *Trends in Ecology and Evolution* (Vol. 18, Issue 6, pp. 299–305). Elsevier Ltd. [https://doi.org/10.1016/S0169-5347\(03\)00071-5](https://doi.org/10.1016/S0169-5347(03)00071-5)

Li, Y., Liao, Q., Li, X., Liao, S., Chi, G., & Peng, S. (2003). Towards an operational system for regional-scale rice yield estimation using a time-series of Radarsat ScanSAR images.

*International Journal of Remote Sensing*, 24(21), 4207–4220.

<https://doi.org/10.1080/0143116031000095970>

Loranty M M and Goetz S J 2012 Shrub expansion and climate feedbacks in Arctic tundra

*Environ. Res. Lett.* 7011005. [https://iopscience.iop.org/article/10.1088/1748-](https://iopscience.iop.org/article/10.1088/1748-9326/7/1/011005/meta)

[9326/7/1/011005/meta](https://iopscience.iop.org/article/10.1088/1748-9326/7/1/011005/meta)

Malhi, Y., Franklin, J., Seddon, N., Solan, M., Turner, M. G., Field, C. B., & Knowlton, N.

(2020). Climate change and ecosystems: Threats, opportunities and solutions. In

*Philosophical Transactions of the Royal Society B: Biological Sciences* (Vol. 375, Issue

1794). Royal Society Publishing. <https://doi.org/10.1098/rstb.2019.0104>

Mann, D., Rupp, T., Olson, M., & Duffy, P. (2012). Is Alaska's Boreal forest now crossing a

major ecological threshold? *Arctic, AntArctic, and Alpine Research*, 44(3), 319–331.

<https://doi.org/10.1657/1938-4246-44.3.319>

McDowell, 2016: Economic impact of Alaska's visitor industry: 2014–15 update. Alaska

Department of Commerce, Community, and Economic Development Rep., 11 pp.,

Mekonnen, Z. A., Riley, W. J., Berner, L. T., Bouskill, N. J., Torn, M. S., Iwahana, G.,

Breen, A. L., Myers-Smith, I. H., Criado, M. G., Liu, Y., Euskirchen, E. S., Goetz, S. J.,

Mack, M. C., & Grant, R. F. (2021). Arctic tundra shrubification: a review of

mechanisms and impacts on ecosystem carbon balance. In *Environmental Research*

*Letters* (Vol. 16, Issue 5). IOP Publishing Ltd. <https://doi.org/10.1088/1748-9326/abf28b>

Melvin, T. (2019, January 20). *Refuge notebook: Laying a foundation for a Biologically Richer*

*World*. Peninsula Clarion. Retrieved April 6, 2022, from

<https://www.peninsulaclarion.com/sports/refuge-notebook-laying-a-foundcation-for-a>

[biologically-richer-world/](https://www.peninsulaclarion.com/sports/refuge-notebook-laying-a-foundcation-for-a-biologically-richer-world/)

- Morton, J. M., Berg, E., Newbould, D., Maclean, D., & O'brien, L. (2006). *Wilderness Fire Stewardship on the Kenai National Wildlife Refuge, Alaska* (Vol. 12, Issue 1).
- Pastick, N. J., Jorgenson, M. T., Goetz, S. J., Jones, B. M., Wylie, B. K., Minsley, B. J., Genet, H., Knight, J. F., Swanson, D. K., & Jorgenson, J. C. (2019). Spatiotemporal remote sensing of ecosystem change and causation across Alaska. *Global Change Biology*, 25(3), 1171–1189. <https://doi.org/10.1111/gcb.14279>
- Peng, C., Ma, Z., Lei, X., Zhu, Q., Chen, H., Wang, W., Liu, S., Li, W., Fang, X., & Zhou, X. (2011). A drought-induced pervasive increase in tree mortality across Canada's Boreal forests. *Nature Climate Change*, 1(9), 467–471. <https://doi.org/10.1038/nclimate1293>
- Petersen, S. L., Stringham, T. K., & Laliberte, A. S. (2005). Classification of willow species using large-scale aerial photography. *Rangeland Ecology and Management*, 58(6), 582–587. <https://doi.org/10.2111/04-129R1.1>
- Prather, C. M., Pelini, S. L., Laws, A., Rivest, E., Woltz, M., Bloch, C. P., del Toro, I., Ho, C. K., Kominoski, J., Newbold, T. A. S., Parsons, S., & Joern, A. (2013). Invertebrates, ecosystem services and climate change. *Biological Reviews*, 88(2), 327–348. <https://doi.org/10.1111/brv.12002>
- Schuck, A., Päivinen, R., Häme, T., van Brusselen, J., Kennedy, P., & Folving, S. (2003). Compilation of a European forest map from Portugal to the Ural mountains based on earth observation data and forest statistics. *Forest Policy and Economics*, 5(2), 187–202. [https://doi.org/10.1016/S1389-9341\(03\)00024-8](https://doi.org/10.1016/S1389-9341(03)00024-8)
- Soja, A. J., Tchebakova, N. M., French, N. H. F., Flannigan, M. D., Shugart, H. H., Stocks, B. J., Sukhinin, A. I., Parfenova, E. I., Chapin, F. S., & Stackhouse, P. W. (2007). Climate induced Boreal forest change: Predictions versus current observations. *Global and*

*Planetary Change*, 56(3–4), 274–296. <https://doi.org/10.1016/j.gloplacha.2006.07.028>

Tape KD, Gustine D D, Ruess R W, Adams L Gand Clark J A 2016 Range expansion of moose in Arctic Alaska linked to warming and increased shrub habitat PLoS One 11e0152636. <https://doi.org/10.1371/journal.pone.0152636>

Turner, M. G., Calder, W. J., Cumming, G. S., Hughes, T. P., Jentsch, A., LaDeau, S. L., Lenton, T. M., Shuman, B. N., Turetsky, M. R., Ratajczak, Z., Williams, J. W., Williams, A. P., & Carpenter, S. R. (2020). Climate change, ecosystems and abrupt change: Science priorities. In *Philosophical Transactions of the Royal Society B: Biological Sciences* (Vol. 375, Issue 1794). Royal Society Publishing. <https://doi.org/10.1098/rstb.2019.0105>

Warszawski, L., Friend, A., Ostberg, S., Frieler, K., Lucht, W., Schaphoff, S., Beerling, D., Cadule, P., Ciais, P., Clark, D. B., Kahana, R., Ito, A., Keribin, R., Kleidon, A., Lomas, M., Nishina, K., Pavlick, R., Rademacher, T. T., Buechner, M., ... Schellnhuber, H. J. (2013). A multi-model analysis of risk of ecosystem shifts under climate change. *Environmental Research Letters*, 8(4). <https://doi.org/10.1088/1748-9326/8/4/044018>

TABLES AND FIGURES

**Table 1.** Confusion matrices for the 2019 classification. Confusion matrices are reported for accuracy assessments performed using both the ‘gridded’ (fishnet) validation method and ‘ground-truth’ validation method. User’s Accuracy and Producer’s Accuracy are reported, with the overall accuracy outlined in black.

**GRIDDED ASSESSMENT**

Class	Tree	Shrub	Grass	Snow	Total Points	User's Accuracy	Kappa
<b>Tree</b>	83	0	0	0	83	100%	0
<b>Shrub</b>	0	76	0	0	76	100%	0
<b>Grass</b>	0	2	78	2	82	95.1%	0
<b>Snow</b>	0	0	5	40	45	88.9%	0
<b>Total Points</b>	83	78	83	42	286	0	0
<b>Producer's Accuracy</b>	100%	97.4%	93.9%	95.2%	0	96.8%	0
<b>Kappa</b>	0	0	0	0	0	0	0.96

**GROUND-TRUTH ASSESSMENT**

Class	Tree	Shrub	Grass	Snow	Total Points	User's Accuracy	Kappa
<b>Tree</b>	86	0	0	0	86	100%	0
<b>Shrub</b>	3	47	0	0	50	94%	0
<b>Grass</b>	6	48	90	7	151	59.6%	0
<b>Snow</b>	1	0	10	53	64	82.8%	0
<b>Total Points</b>	96	95	100	60	351	0	0
<b>Producer's Accuracy</b>	89.6%	49.5%	90%	88.3%	0	78.6%	0
<b>Kappa</b>	0	0	0	0	0	0	0.71

**Table 2.** Confusion matrices assessing accuracy for the 2021 imagery classification, without aggregation applied. Confusion matrices are reported for accuracy assessments performed using both the ‘gridded’ (fishnet) validation method and ‘ground-truth’ validation method. User’s Accuracy and Producer’s Accuracy are reported, with the overall accuracy outlined in black.

<b>GRIDDED ASSESSMENT</b>						
<b>Class</b>	<b>Tree</b>	<b>Shrub</b>	<b>Grass</b>	<b>Total Points</b>	<b>User's Accuracy</b>	<b>Kappa</b>
<b>Tree</b>	55	0	1	56	98.2%	0
<b>Shrub</b>	9	59	3	71	83.1%	0
<b>Grass</b>	1	6	61	68	89.7%	0
<b>Total Points</b>	65	65	65	195	0	0
<b>Producer's Accuracy</b>	84.6%	90.8%	93.8%	0	89.7%	0
<b>Kappa</b>	0	0	0	0	0	0.85

<b>GROUND-TRUTH ASSESSMENT</b>						
<b>Class</b>	<b>Tree</b>	<b>Shrub</b>	<b>Grass</b>	<b>Total Points</b>	<b>User's Accuracy</b>	<b>Kappa</b>
<b>Tree</b>	68	1	1	70	97.10%	0
<b>Shrub</b>	12	85	0	97	87.60%	0
<b>Grass</b>	11	5	89	105	84.80%	0
<b>Total Points</b>	91	91	90	272	0	0
<b>Producer's Accuracy</b>	74.7%	93.4%	98.9%	0	89.0%	0
<b>Kappa</b>	0	0	0	0	0	0.83

**Table 3.** Confusion matrices for the 2021 classification. Confusion matrices are reported for accuracy assessments performed using both the ‘gridded’ (fishnet) validation method and ‘ground-truth’ validation method with aggregation applied (top two matrices), and without aggregation applied (bottom two matrices). User’s Accuracy and Producer’s Accuracy are reported, with the overall accuracy outlined in black.

**2021 GRIDDED ASSESSMENT (WITH AGGREGATION)**

Class	Tree	Shrub	Grass	Total Points	User's Accuracy	Kappa
Tree	44	3	6	53	83.0%	0
Shrub	16	52	2	70	74.3%	0
Grass	5	10	57	72	79.2%	0
Total Points	65	65	65	195	0.0%	0
Producer's Accuracy	67.7%	80.0%	87.7%	0.0%	78.5%	0.0%
Kappa	0	0	0	0	0.0%	0.68

**2021 GRIDDED ASSESSMENT (WITH AGGREGATION)**

Class	Tree	Shrub	Grass	Total Points	User's Accuracy	Kappa
Tree	47	0	0	47	100.0%	0
Shrub	25	73	0	98	74.5%	0
Grass	19	18	90	127	70.9%	0
Total Points	91	91	90	272	0.0%	0
Producer's Accuracy	51.6%	80.2%	100%	0.0%	77.2%	0.0%
Kappa	0	0	0	0	0.0%	0.66

**2021 GRIDDED ASSESSMENT (WITH NO AGGREGATION)**

Class	Tree	Shrub	Grass	Total Points	User's Accuracy	Kappa
Tree	55	0	1	56	98.2%	0
Shrub	9	59	3	71	83.1%	0
Grass	1	6	61	68	89.7%	0
Total Points	65	65	65	195	0.0%	0
Producer's Accuracy	84.6%	90.8%	93.8%	0.0%	89.7%	0.0%
Kappa	0	0	0	0	0.0%	0.85

**2021 GROUND ASSESSMENT (WITH NO AGGREGATION)**

Class	Tree	Shrub	Grass	Total Points	User's Accuracy	Kappa
Tree	68	1	1	70	97.1%	0
Shrub	12	85	0	97	87.6%	0
Grass	11	5	89	105	84.8%	0
Total Points	91	91	90	272	0.0%	0
Producer's Accuracy	74.7%	93.4%	98.9%	0.0%	89.0%	0.0%
Kappa	0	0	0	0	0.0%	0.83

**Table 4.** Percent Cover of each class for the 2019 classification, the 2021 classification with aggregation, and the 2021 classification without aggregation. Snow was not present during the collection of the 2021 imagery.

Class	Percent Coverage		
	2019	2021	
		<i>w/aggregation</i>	<i>w/out aggregation</i>
Tree	3.13%	2.75%	7.25%
Shrub	25.31%	29.61%	34.38%
Grass	67.43%	67.65%	58.36%
Snow	4.12%	0%	0%



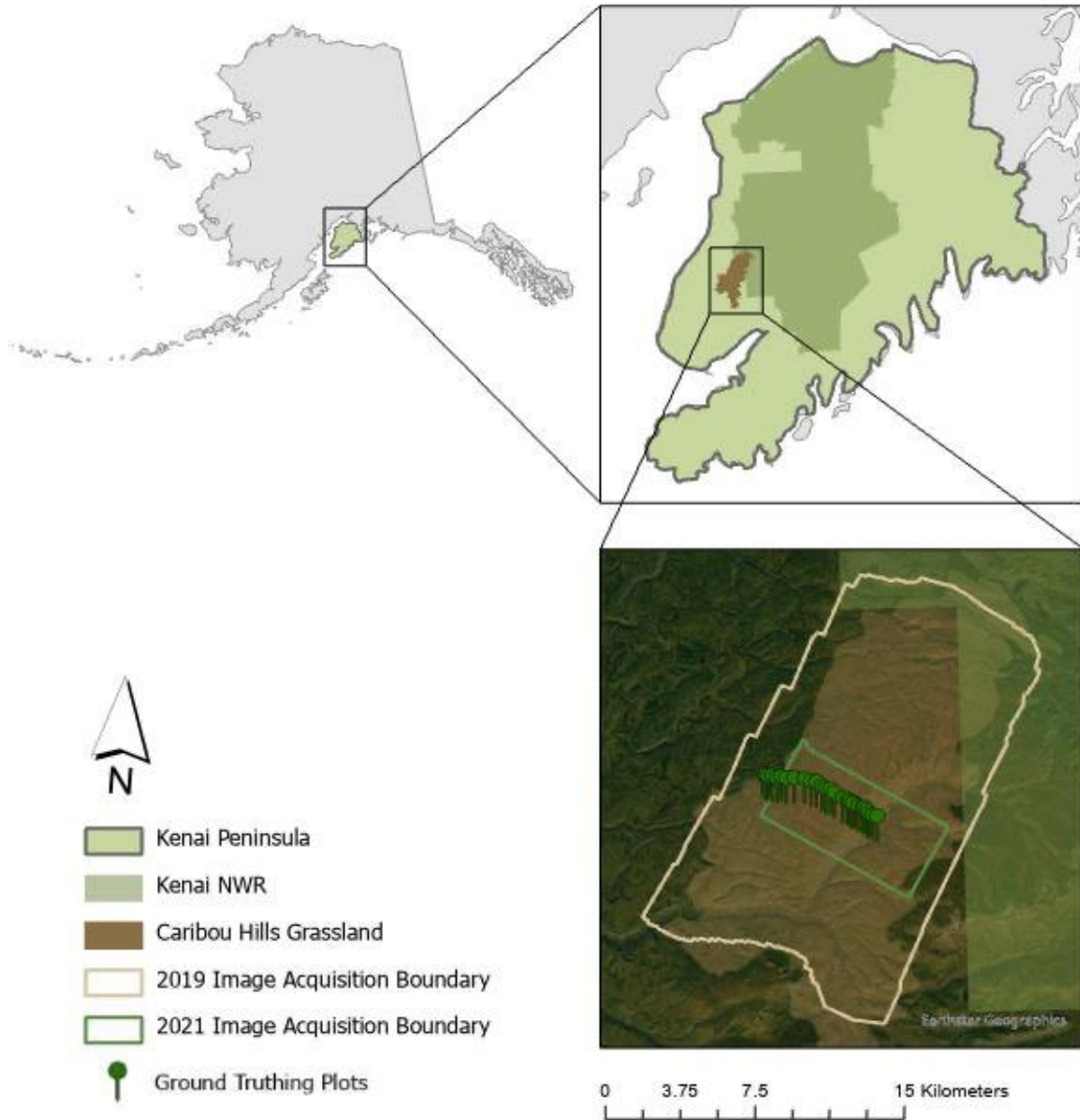


**Figure 1.** Location of the Kenai Peninsula in Alaska, United States. The Caribou Hills Grassland is located in the west-central portion of the Kenai Peninsula on the western boundary of the Kenai National Wildlife Refuge (*upper right*), with the 2019 and 2021 imagery acquisition boundaries within the Caribou Hills Grassland (*lower right*). Locations of ground-truthed plots within the 2021 image acquisition boundary are depicted by green pins.

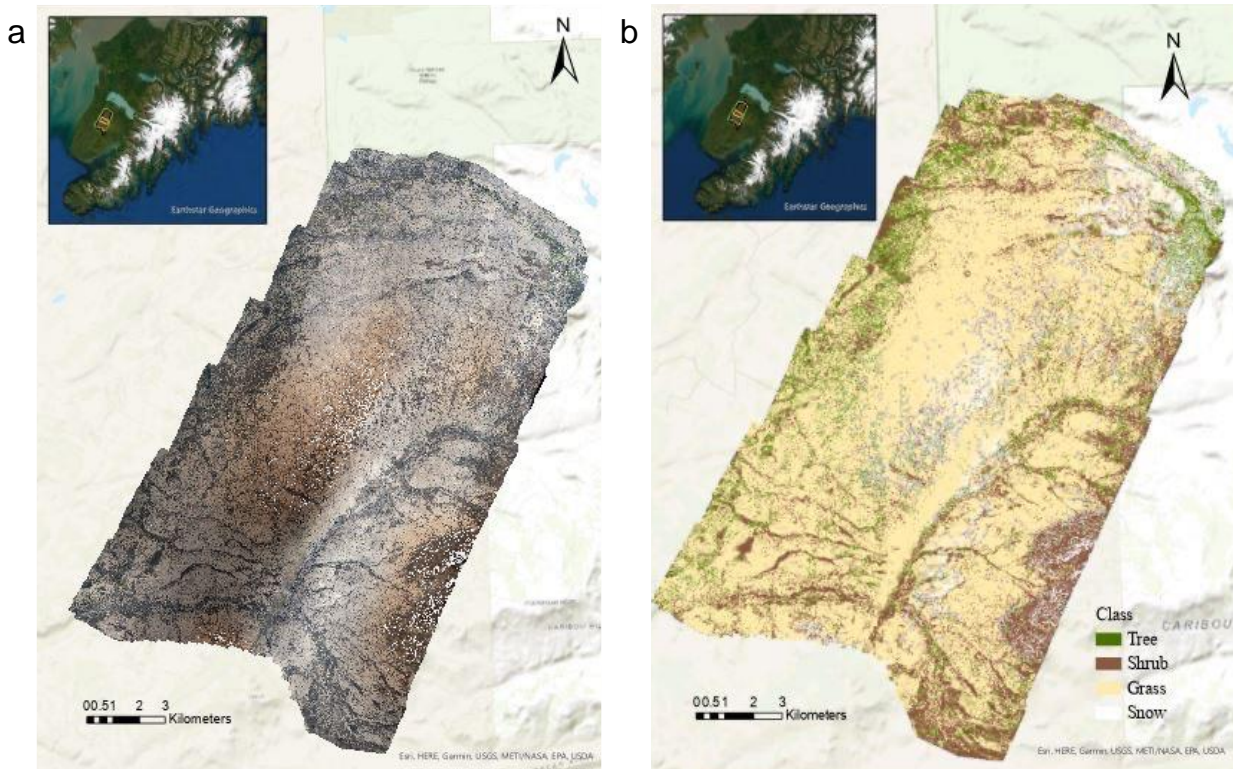


**Figure 2.** (a) 2019 RGB aerial imagery acquired at 0.1 m (10 cm) resolution. (b) 2019 land cover classification of the aerial imagery with a resolution of 0.3 m (30 cm). Land cover classes include tree, in green; shrub, in brown; grass, in yellow; and snow, in white.

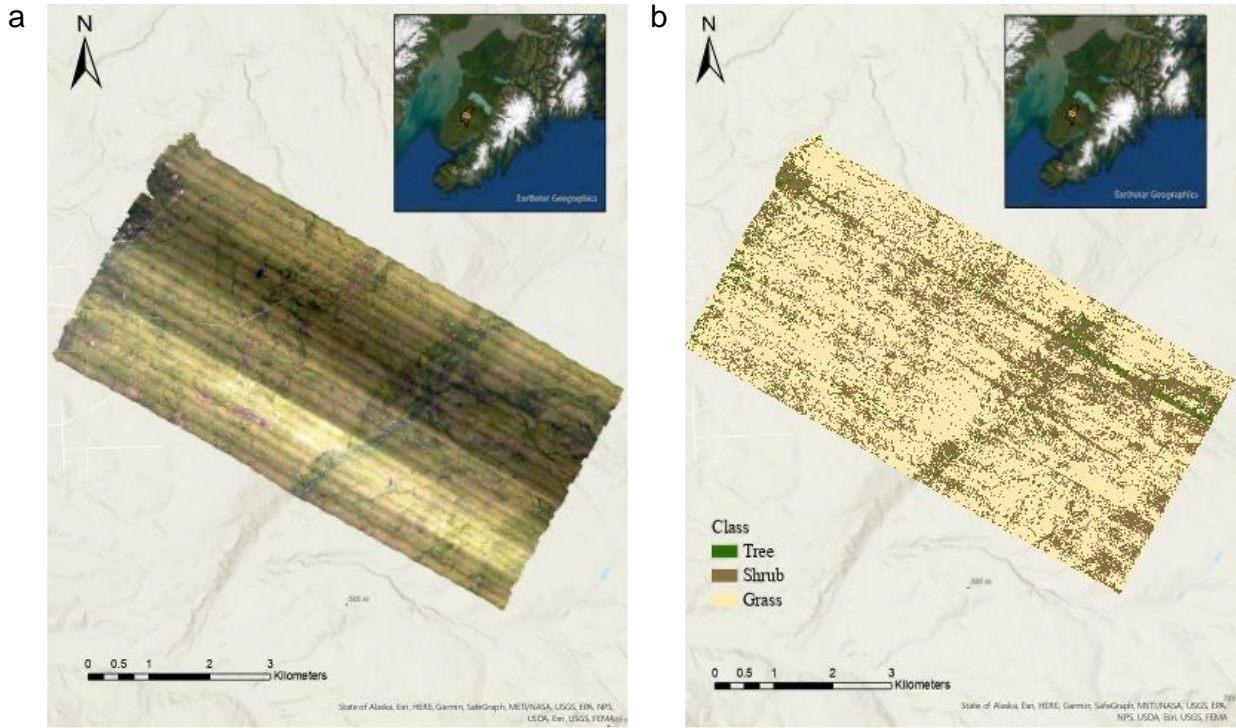


**Figure 3.** (a) 2021 RGB aerial imagery acquired at 0.05 m (5 cm) resolution. (b) 2021 land cover classification of the aerial imagery with a resolution of 0.2 m (20 cm). Land cover classes include tree, in green; shrub, in brown; and grass, in yellow.

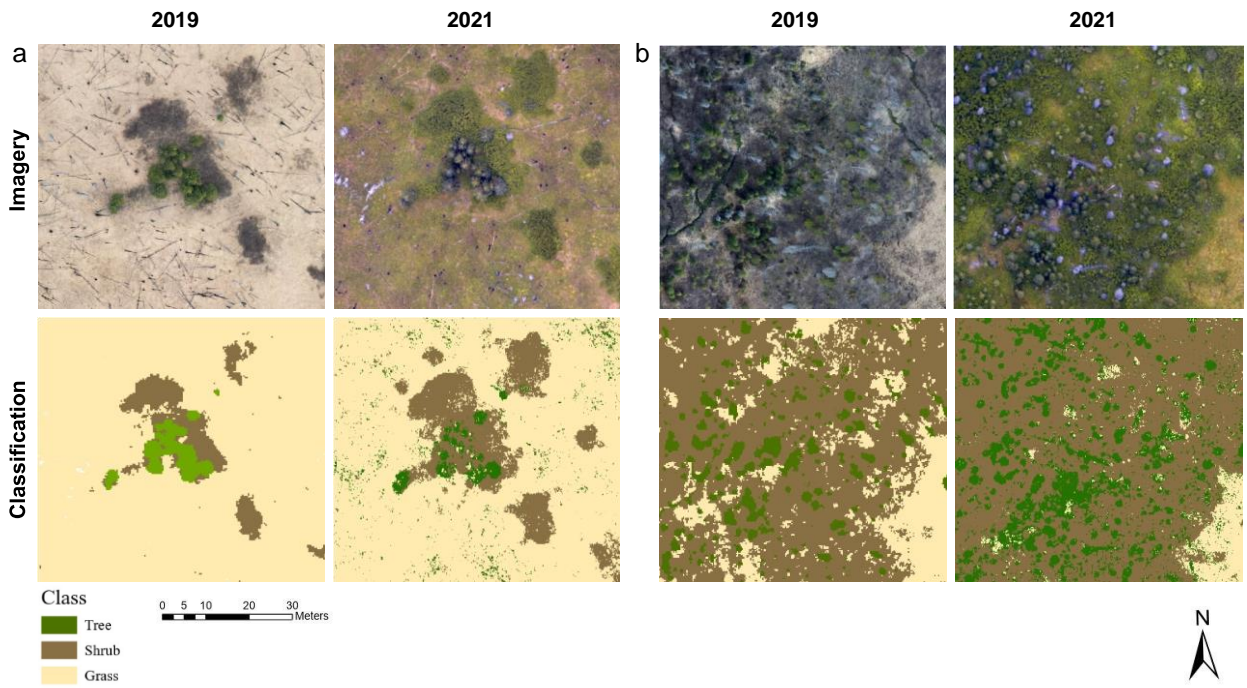


**Figure 4.** (a) Comparison of the 2019 and 2021 imagery and corresponding classifications from an area with sparse vegetation cover; and (b) Comparison of the 2019 and 2021 imagery and corresponding classifications from an area with dense vegetation cover.

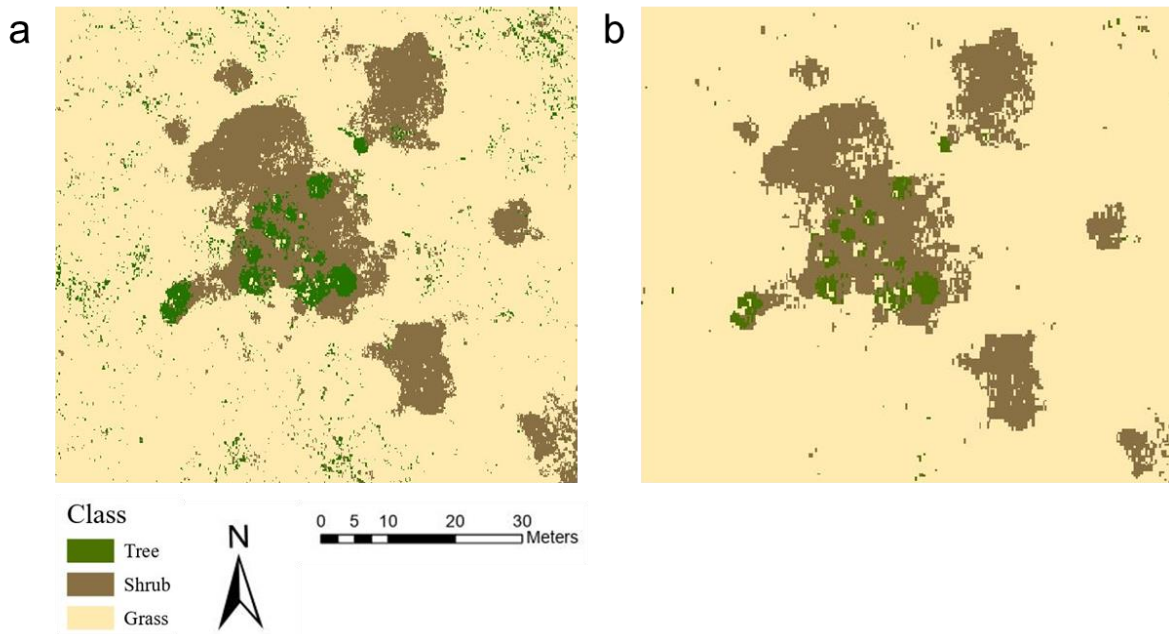


**Figure 5.** A comparison of the classification with and without the aggregation effect (a) zoomed-in area of the 2021 classification without aggregation (5 cm resolution) (b) zoomed-in area of the 2021 with aggregation (cell factor: 6, aggregation technique: maximum resulting in 20 cm resolution).

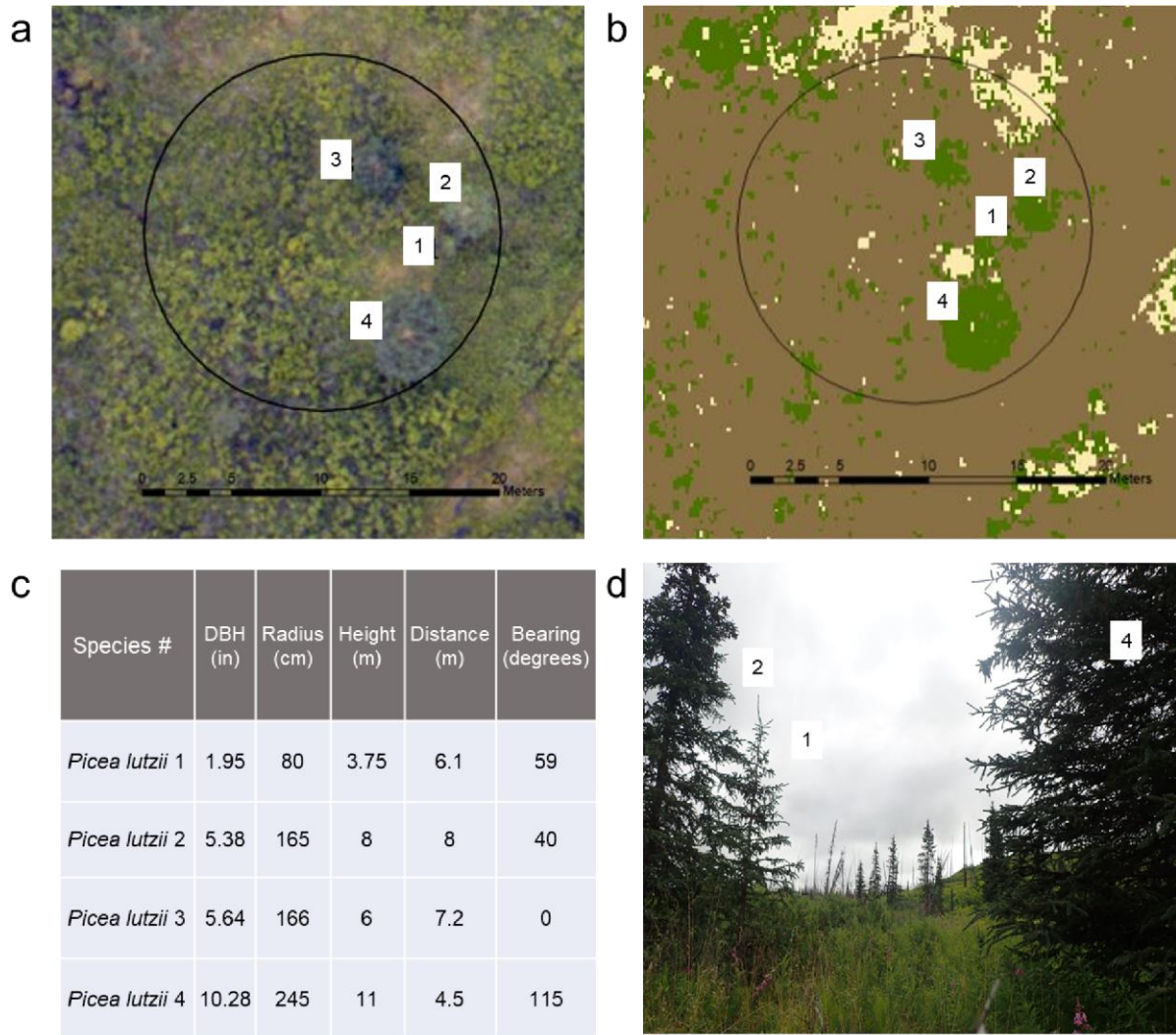


**Figure 6.** An example of data from ground-truth plot 24 collected during August 2021 (a) 2021 imagery with plot 24, including a 10-m radius plot drawn, and four trees labeled that were ground-truthed (b) Classification of plot 24 with four labeled trees that were ground-truthed (c) Data collected on the ground for each recorded tree; includes species and number, DBH, tree canopy radius, height, distance from plot center, and tree bearing from plot center (d) Photograph taken on the ground from plot center in the eastern direction, capturing trees 1, 2 and 4 (tree 3 was not visible while facing east, but was captured in the north facing image).

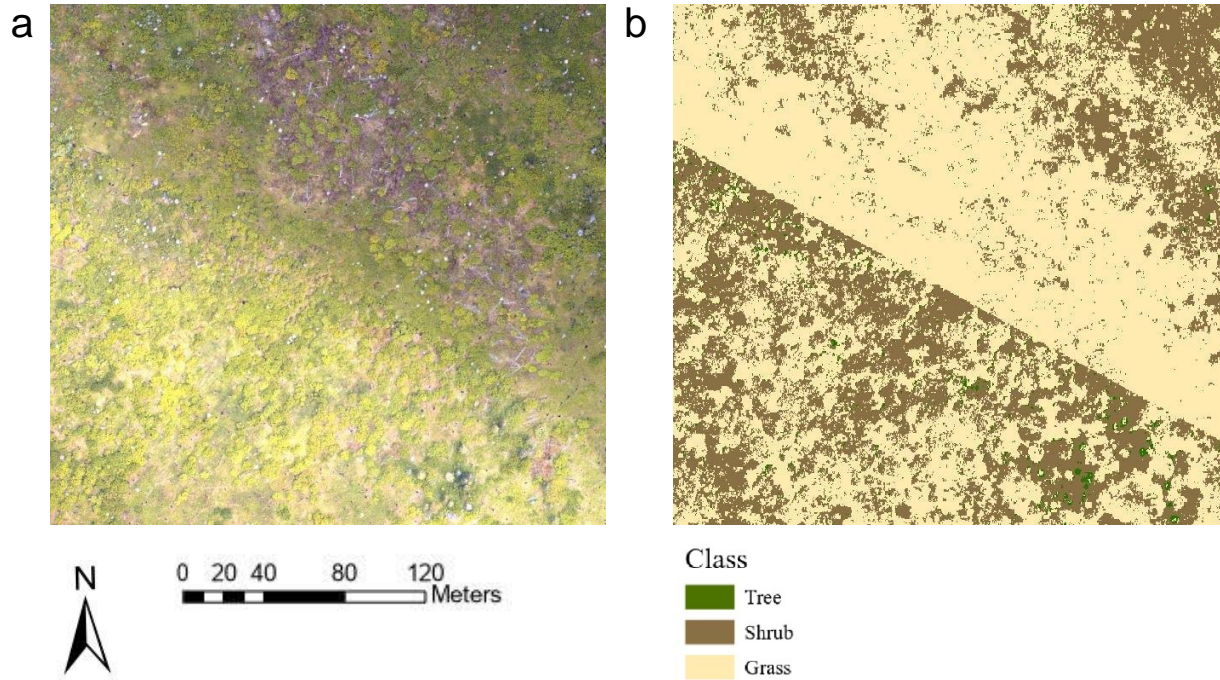


**Figure 7.** A comparison of 2021 imagery and classification along a polygon boundary where exposure changed drastically (a) 2021 zoomed-in imagery (b) 2021 zoomed-in classification of the same area.